



Citation for published version:

Ge, S, Xu, Z, Liu, H, Gu, C & Li, F 2019, 'Flexibility evaluation of active distribution networks considering probabilistic characteristics of uncertain variables', *IET Generation, Transmission and Distribution*, vol. 13, no. 14, pp. 3148-3157. <https://doi.org/10.1049/iet-gtd.2019.0181>

DOI:

[10.1049/iet-gtd.2019.0181](https://doi.org/10.1049/iet-gtd.2019.0181)

Publication date:

2019

Document Version

Peer reviewed version

[Link to publication](#)

© 2019 IEEE. Personal use of this material is permitted. Permission from IEEE must be obtained for all other users, including reprinting/ republishing this material for advertising or promotional purposes, creating new collective works for resale or redistribution to servers or lists, or reuse of any copyrighted components of this work in other works.

University of Bath

General rights

Copyright and moral rights for the publications made accessible in the public portal are retained by the authors and/or other copyright owners and it is a condition of accessing publications that users recognise and abide by the legal requirements associated with these rights.

Take down policy

If you believe that this document breaches copyright please contact us providing details, and we will remove access to the work immediately and investigate your claim.

Flexibility Evaluation of Active Distribution Networks considering Probabilistic Characteristics of Uncertain Variables

Shaoyun Ge¹, Zhengyang Xu¹, Hong Liu^{1*}, Chenghong Gu², Furong Li²

¹ Key Laboratory of Smart Grid of Ministry of Education, Tianjin University, No. 92 Weijin Road, Tianjin, People's Republic of China

² Department of Electronic and Electrical Engineering, University of Bath, BA2 7AY, Bath, UK

*liuhong@tju.edu.cn

Abstract: The flexibility evaluation of distribution networks has attracted significant research attention with the increasing penetration of renewable energy (RE). One particular gap in existing studies is that little attention has been paid to the probabilistic characteristics of uncertain regions. In this paper, a novel sequential flexibility evaluation method is proposed based on the feasibility analysis of the uncertain region of photovoltaic active power (PVAP) and load demand. The model features the uncertain region with probabilistic characteristics, which is essential for analysing the impact of probabilistic characteristics of uncertain variables (PCUV) on flexibility evaluation. The sequential direction matrix is adopted to reflect the major factor of flexibility shortage. The evaluation procedure is modelled as a bi-level optimization problem. Demonstrated by the simulation results, the flexibility index is larger by considering the PCUV. Furthermore, the elements in the sequential direction matrix indicate that the photovoltaic power during midday is the major cause of flexibility shortage.

Nomenclature

A. Indices

i, j	Node i, j
l	Line l
t	Time t
n	Uncertain variable n

B. Variables

D	Sequential direction matrix
P_{PV}	Photovoltaic active power (PVAP)
P_{PV}^N	Predicted PVAP
ΔP_{PV}	Prediction error of the PVAP
u, u^{exp}	Uncertain variable and its expectation
δ	Scaled deviation
Δu	Difference between uncertain variables' maximum/minimum deviation and its expectation.
F	Flexibility index
φ^D	Probability-weighted maximum feasible deviation in direction D
δ^D	Maximum feasible deviation in direction D
ω^D	Weight of boundary point of the feasible region in direction D
$P_{n,t}$	Probability sequence of uncertain variable n
i^D	Probability sequence's serial number of feasible region's boundary point in direction D
δ	Scaled deviation
x	Decision variables of the optimization
P_i, Q_i	Active power and reactive power injected at node i
U_i, U_j	Voltage amplitude of node i and node j
I_l	Current of line l
$P_{DGi,t}, Q_{DGi,t}$	Active/reactive power output of distributed generation at node i
$E_{SOC,t}$	State of Charge of the energy storage battery

$u_{c,t}, u_{d,t}$	Charging and discharging flags
$p_{c,t}, p_{d,t}$	Actual charging and discharging power

C. Parameters

ΔP_{PV}	Step size of discretization
$P_{PV,t}^{\text{max}}, P_{PV,t}^{\text{min}}$	Maximum and minimum PVAP
T	Total number of time intervals
N	Total number of uncertain variables
G_{ij}, B_{ij}	Conductance and susceptance between node i and node j
I_l^{max}	Maximum current of line l
$U_{i \text{max}}, U_{i \text{min}}$	Maximum and minimum voltage limit
S_{DGi}	DG inverter capacity at the node i of the network
$E_{SOC,\text{min}}, E_{SOC,\text{max}}$	Minimum of SOC Maximum of SOC
$p_{c \text{max}}, p_{d \text{max}}$	Maximum charging and discharging power
η_c	Charging efficiency of ESS
η_d	Discharging efficiency
Δt	Charging/discharging time intervals

D. Abbreviations

RE	Renewable energy
PVAP	Photovoltaic active power
REOP	Renewable energy output power
PCUV	Probabilistic characteristics of uncertain variables
BA	Bisection algorithm

1. Introduction

1.1. Motivation

Distribution networks with high-penetration of renewable energy (RE) are a critical measure to fight environmental pollutions and energy crisis [1-2]. The uncertainty from high-penetration of RE together with the uncertainty of electricity consumption, results in bi-uncertain characteristics of both

supply and demand side of distribution networks [3]. The distribution network is required to have the ability to effectively cope with multiple uncertainties in the operation [4-5]. Thus, a more flexible distribution network is required.

1.2. Literature review

The definition of distribution network flexibility has been drawing extensive attention [6]. The studies on distribution network flexibility originate from power system flexibility [7, 8]. The flexibility was defined in [9] as “flexibility expresses the extent to which a power system can modify its electricity production and consumption in response to variability, expected or otherwise.” Nosair *et al.* [10] proposed the method of flexibility envelope to evaluate the flexibility potential of power systems. Zhao *et al.* [11] constructed a flexibility metric to reflect the largest variation range of uncertainty that a system can withstand. Mueller *et al.* proposed the aggregation model of flexibility resources based on zonotopic sets [12]. An algorithm that distributes aggregate-level control decisions among individual systems of the population in an economically fair way was introduced [13]. The abovementioned works have evaluated the flexibility in power systems via zonotopic sets or variation range envelopes, which focus on ramping shortage caused by considerable volatility and uncertainty of renewable energy output power (REOP).

RE is normally integrated into the distribution network in a distributed way. From the network perspective, the critical constraints include nodal voltage, branch current etc, which are essentially different from the ramping issues of power systems [14]. Regarding the flexibility evaluation for distribution networks, an index system that pertains to particular aspects of distribution networks was proposed in [15]. Majzoubi *et al.* suggested [16] that distribution net load variability should be considered in the flexibility evaluation for distribution networks. Thus, a flexibility-oriented microgrid optimal scheduling model was developed. Ji *et al.* [17] evaluated the flexibility of SOP integration by the maximum RE hosting capacity. Xiao *et al.* [18] defined the flexible distribution network and presented the normal operation mode, $N-1$ mode, and related analysis methods. In the existing studies, only the volatility of REOP and load demand are investigated, but the uncertainty from forecasting error is not considered. Thus, the abovementioned methods can only be applied to deterministic problems.

From the probabilistic perspective, the mathematical description of power system flexibility at planning stage based on probability theory was introduced in [19]. Lu *et al.* [20] proposed a probabilistic flexibility evaluation method for power system planning based on the relationship between flexibility and renewable energy curtailment. In [19, 20], the probability distribution of flexibility adequacy was calculated statistically in a long time scale, which is not valid for sequential flexibility evaluation in a short time scale. On the other hand, the uncertain variables were the actual REOP in the target year of power system planning, but, the prediction errors of REOP in sequential operation have not been considered.

Generally, the aforementioned studies on flexibility evaluation have not yet considered the prediction error of REOP as uncertain variables, and the probabilistic characteristics of prediction error have been ignored. Wan *et al.* [21] proposed a novel set-based method to formulate the

maximum uncertainty boundary of distributed generation uncertainties. Research in other domain [22] adopted hyper-rectangle to describe multi-dimensional space of uncertain variables. However, probabilistic characteristics of uncertain regions are ignored in [21] and [22]. Based on the above analysis, the definition and scope of distribution network flexibility should be determined first and applicable flexibility evaluation method should be proposed.

1.3. Contributions

In this paper, a flexibility evaluation method for distribution networks considering the probability distribution of uncertain variables is proposed. The flexibility of distribution networks is quantified based on the feasibility analysis of uncertain regions of photovoltaic active power (PVAP) and load power. The contributions of this work are as follows.

1) We characterize the feasibility of uncertain regions with probabilistic characteristics for the flexibility evaluation of distribution networks. This helps to quantify the distribution network’s capability to cope with multiple uncertainties.

2) The sequential direction matrix is adopted to capture the temporal characteristics of uncertain variables, which is essential for recognizing the major factors of flexibility shortage.

3) According to the case study, the weighted flexibility index is larger than the ordinary flexibility index. It reflects the impact of PCUV on flexibility evaluation, since the probability of points in the centre of the uncertain region is higher than other points. In a sequential direction matrix, the larger elements indicate more severe violations of the nodal voltage constraint.

1.4. Paper organization

The rest of the paper is organized as follows. Section 2 presents the definition and research framework of distribution network flexibility. Section 3 develops a bi-level weighted flexibility evaluation model. Section 4 presents the solution algorithm for the proposed model. In Section 5, the case study presents the flexibility evaluation results of ordinary flexibility and weighted flexibility. Section 6 concludes the paper.

2. Definition of distribution network flexibility

To date, little attention in literature has been devoted to the uncertain region and its probabilistic characteristics. Thus the definition of distribution network flexibility is first defined and then, the outline of the proposed flexibility evaluation method is described.

2.1. The flexibility of the distribution network

Under the context of large-scale RE integrated into the distribution network, flexibility is employed to quantify the distribution network’s adaptability to uncertain variables, which are from RE prediction errors and load prediction errors. All sources of uncertainties are called flexibility requirement. All resources to cope with volatility and uncertainty are called flexibility resources, including nodal flexibility resources [23, 24] and network flexibility resources [25].

In this paper, the distribution network flexibility is defined as: the ability that a distribution network has to effectively cope with multiple uncertainties in the operation, to: i) adapt

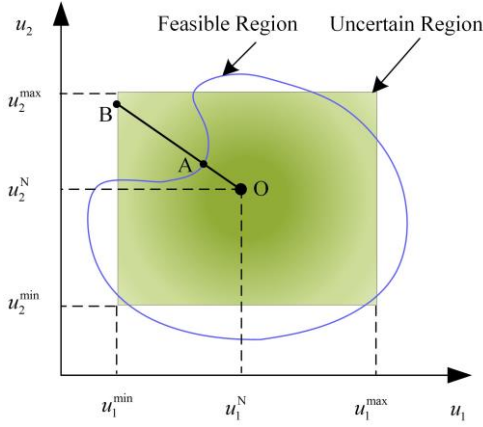


Fig. 1. Schematic diagram of proposed flexibility evaluation method

to various complex operating environment, ii) maintain high-level operational targets by full coordination, iii) utilize adjustable resources in the system. The flexibility of distribution networks can be quantified based on the feasibility analysis of uncertain regions. Specifically, the quantification of flexibility can be realized by recognizing the critical point of a feasible region in the space of uncertain variables.

Fig.1 shows the schematic diagram of the proposed flexibility evaluation method for the distribution network. Each point in the coordinate system corresponds to a combination of uncertain variables, called operation point. The rectangular region is the uncertain region. The probability of points in the centre of the region is higher, represented by the darker colour in this area. The region bounded by the closed curve is a feasible region. For the operation points inside the feasible region, a feasible operation scheme can be obtained by optimally scheduling resources in distribution networks. For the operation points outside, no feasible operation schemes can be obtained due to constraint violation.

As demonstrated in Fig. 1, point O is an expected point, representing the combination of predicted uncertain variables. For any direction from point O in the uncertain space, the boundary point of the feasible region and uncertain region can be both determined, where the weighted maximum feasible deviation at direction D is denoted by φ^D (Equation (8)). Among all the directions in the uncertain space, there is one direction with the minimum φ^D , which is the flexibility index F . This direction is the critical direction, and the boundary point of the feasible region at this direction is the critical point (point A in Fig.1). When uncertain variables are extended from 2-dimension to n-dimension, the uncertain region is accordingly extended to a hyper-rectangle of n-dimension.

2.2. Research framework of flexibility evaluation

In this paper, the proposed flexibility evaluation model for the sequential operation of distribution networks includes a master problem and a subproblem. The master problem searches the critical direction in the uncertain space, and the decision variable of the master problem is sequential direction matrix. The subproblem includes an upper layer and a lower layer. The upper layer searches the boundary point of the feasible region. The lower layer is based on a feasibility analysis of the boundary point and the result is returned to the

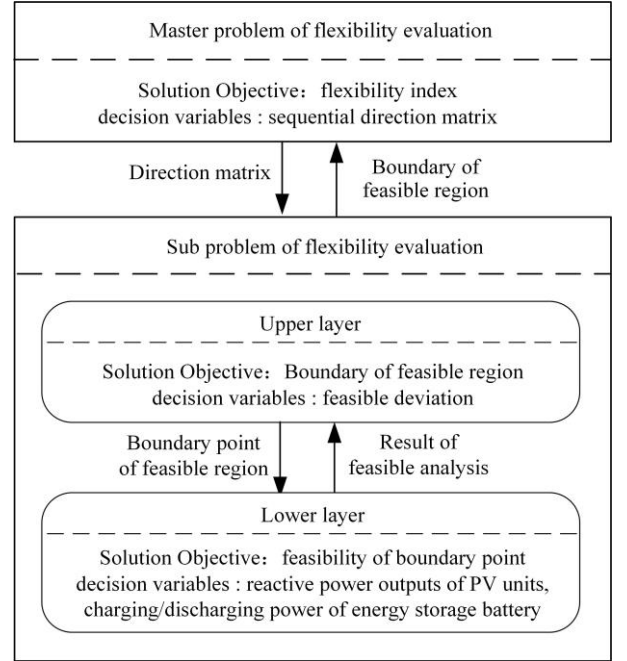


Fig. 2. The proposed approach for flexibility evaluation

upper layer. In this paper, the validation of the proposed model is demonstrated by taking nodal flexibility resources such as PV units and energy storage system (ESS). At the lower layer of the subproblem, decision variables are reactive power outputs of PV units [26-28] and charging/discharging power of ESS. When the bisection algorithm converges, the boundary point of the feasible region in a particular direction is returned to the master problem. With multiple iterations, the critical point and critical direction can be obtained by the master-problem.

3. Mathematics model

In the flexibility evaluation process for the distribution network, a weighted maximum feasible deviation is calculated. The critical point and critical direction in n-dimension space can be obtained. Uncertain variables are treated as probability sequences, and the sequential direction matrix is introduced to describe any directions in the n-dimension space. Accordingly, the flexibility evaluation model of the distribution network is formulated.

3.1. Probability model

A major problem with the evaluation method in [22] is that the probability anywhere in an uncertain region is assumed to be the same. Due to this, neither the probability distribution characteristics nor the impact of the characteristics on flexibility evaluation results are reflected. Therefore, the probability models of PV power and load demand are formulated based on probability sequence [29, 30]. Thereafter, an uncertain region for flexibility evaluation is obtained.

3.1.1 Probabilistic sequence: The probabilistic sequence is defined as: a discrete sequence $a(i)$, $i=0,1,\dots,N_a$ with a fixed length N_a , if $0 \leq a(i) \leq 1$, and $\sum_{i=0}^{N_a} a(i) = 1$. The sequence is called a probabilistic sequence.

3.1.2 Probabilistic sequence of PV power: At a given time t , the PVAP can be expressed as the sum of predicted value and prediction error.

$$P_{PV}(t) = P_{PV}^N(t) + \Delta P_{PV}(t) \quad (1)$$

where $P_{PV}(t)$ is the PVAP at time t , $P_{PV}^N(t)$ is the predicted PVAP at time t , $\Delta P_{PV}(t)$ is the prediction error of the PVAP at time t .

$P_{PV}(t)$ is represented by a normal distribution $P_{PV}(t) \sim N(P_{PV}^N(t), \delta_{PV}(t))$. $\delta_{PV}(t)$ is the standard deviation of the normal distribution. The probability density function of the PVAP at time t is formulated as:

$$f_{PV,t}(x) = \frac{1}{\sqrt{2\pi}\delta_{PV}(t)} \exp\left(-\frac{x - P_{PV}^N(t)}{2\delta_{PV}^2(t)}\right) \quad (2)$$

Based on the probability density function of the PV output, the corresponding probability sequence is formulated, denoted as $P_{PV,t}(i_{PV,t})$. The length of the sequence $N_{PV,t}$ is

$$N_{PV,t} = \left\lceil \frac{P_{PV,t}^{\max} - P_{PV,t}^{\min}}{\Delta P_{PV}} \right\rceil \quad (3)$$

where $\lceil a \rceil$ indicates the maximum integer not bigger than a . $P_{PV,t}^{\max}$ is the maximum PVAP at time t , which is usually the installed capacity of PV. $P_{PV,t}^{\min}$ is the minimum PVAP at time t , usually equal to 0. ΔP_{PV} is the step size of discretization. The length of the sequence $N_{PV,t}$ is the number of elements in the discrete probabilistic sequence, corresponding to N_a in Section 3.1.1. It will be compared with $i_{PV,t}$ in (4) to determine the mathematical expression of $P_{PV,t}(i_{PV,t})$.

The sequential probability sequence is formulated as:

$$P_{PV,t}(i_{PV,t}) = \begin{cases} \int_0^{\frac{\Delta P_{PV}}{2}} f_{PV,t}(x) dx & i_{PV,t} = 0 \\ \int_{i_{PV,t}\frac{\Delta P_{PV}}{2}}^{i_{PV,t}\frac{\Delta P_{PV}}{2} + \frac{\Delta P_{PV}}{2}} f_{PV,t}(x) dx & 0 < i_{PV,t} < N_{PV,t} \\ \int_{i_{PV,t}\frac{\Delta P_{PV}}{2}}^{i_{PV,t}\frac{\Delta P_{PV}}{2} - \frac{\Delta P_{PV}}{2}} f_{PV,t}(x) dx & i_{PV,t} = N_{PV,t} \end{cases} \quad (4)$$

where $P_{PV,t}(i_{PV,t})$ is the sequential probability sequence. And $f_{PV,t}(x)$ is the probability density function of the PVAP at time t calculated in (2). ΔP_{PV} is the step size of discretization in (3). $N_{PV,t}$ is the length of the sequence obtained from (3).

Based on (4), the probability sequences of all time periods can be obtained. The sequential probability sequences will be used in (9) to calculate the weight of the feasible region's boundary point.

3.1.3 Probabilistic sequence of load power: Probabilistic sequence of load power is similar to that of PV. To save space, details are not given here.

3.2. Sequential direction matrix

Any operation point in the uncertain space can be expressed by the scaled deviation and its direction. As a result, a critical point can be obtained by searching for critical direction. The flexibility index is then calculated. The critical point can be at any direction of the uncertain space. Consequently, a sequential direction matrix is introduced to describe the directions in an uncertain space.

Regarding the sequential operation problem of distribution networks, uncertain variables vary at different time. For example, the PVAP is zero at night and thus it is no longer an uncertain variable during the night. Therefore, the notion of direction matrix [22] is extended to sequential direction matrix in this paper, expressed as:

$$D = \begin{pmatrix} d_1^1 & d_1^2 & \cdots & d_1^N \\ d_2^1 & d_2^2 & & d_2^N \\ & & \ddots & \\ d_T^1 & d_T^2 & & d_T^N \end{pmatrix} \quad (5)$$

where T is the total number of time intervals. N is the total number of uncertain variables. D is a $T \times N$ sequential direction matrix. The boundary point of the uncertain region at critical direction (point B in Fig.1.) is on the boundary of at least one dimension uncertain variable. As a result, there is at least one element to be 1 or -1. Furthermore, being 1 or -1, the element has a more significant impact on flexibility index than other elements.

In the uncertain space, any operation point can be formulated as:

$$u = u^{\exp} + \delta D \cdot * \Delta u \quad (6)$$

where u and u^{\exp} are the uncertain variable and its expectation. The scaled deviation is denoted by δ . Δu is the difference between uncertain variables' maximum/minimum deviation and its expectation. "*" is the operator of Hadamard product, expressing the multiplication of the corresponding positions of two matrices.

The unified expression of the uncertain variables, u , is used as the input variables in the lower layer of the subproblem. The subproblem searches the maximum feasible deviation (the maximized δ in equation (6)) in a particular direction.

3.3. The master problem

3.3.1 Objective function: A major advantage of the proposed model is that PCUV is considered. The objective function of the master problem is formulated as:

$$F = \min_D \varphi^D \quad (7)$$

where F is the flexibility index, and φ^D is the probability-weighted maximum feasible deviation in direction D . The master problem searches critical direction in the uncertain space. The weighted maximum feasible deviation in critical direction is the flexibility index.

$$\varphi^D = 1 - (1 - \delta^D) \times \omega^D \quad (8)$$

where δ^D is the maximum feasible deviation in direction D . ω^D is the weight of boundary point of the feasible region in direction D , formulated as:

$$\omega^D = \prod_{t=1}^T \prod_{n=1}^N \frac{P_{n,t}(i^D)}{\max(P_{n,t})} \quad (9)$$

where $P_{n,t}$ is the probability sequence of uncertain variable n at time t , and i^D is the probability sequence's serial number of the feasible region's boundary point in direction D .

It is ensured in (9) that the boundary point of the feasible region with higher probability has a larger weight. Furthermore, φ^D is directly proportional to δ^D , while inversely proportional to ω^D . The master problem searches for the minimum probability-weighted maximum feasible deviation, and therefore, the direction with smaller deviation and higher probability is more likely to be the critical direction.

Regarding the flexibility index, if $F > 1$, there are adequate flexibility resources in the distribution network. Being feasible anywhere in the uncertain region, the distribution network is able to endure a wider range of uncertain variables. If $F = 1$, the flexibility resources in the distribution network are just enough for the entire uncertain region. If $F < 1$, the flexibility resources are insufficient in the distribution network due to constraint violation such as branch current limits and voltage limits.

3.3.2 Constraint: The constraint of the master problem is the elements in the sequential direction matrix:

$$-1 \leq d_i^n \leq 1 \quad (10)$$

where, d_i^n is the element of uncertain variable n at time t in the sequential direction matrix.

3.4. The sub problem

3.4.1 Objective function: The objective function of the subproblem is formulated as:

$$\delta^D = \max_x \delta \quad (11)$$

where δ is the scaled deviation, and x is the decision variables of the optimization. The subproblem of flexibility evaluation searches the maximum feasible deviation, i.e., the boundary point of a feasible region in a particular direction.

3.4.2 Constraints on power flow equations: The power flow equations related to active and reactive power injections of nodes are

$$\begin{cases} P_i = U_i \sum_{j \in i} U_j (G_{ij} \cos \theta_{ij} + B_{ij} \sin \theta_{ij}) \\ Q_i = U_i \sum_{j \in i} U_j (G_{ij} \sin \theta_{ij} - B_{ij} \cos \theta_{ij}) \end{cases} \quad (12)$$

where, P_i and Q_i are the active power and reactive power injected at node i , respectively. U_i and U_j are the voltage amplitudes of node i and node j , respectively. G_{ij} and B_{ij} are the conductance and susceptance between node i and node j , respectively. θ_{ij} is the phase difference of voltage between node i and node j .

3.4.3 Constraint on branch flow: The branch power flow constraint is as follows:

$$S_l \leq S_l^{\max} \quad (13)$$

where, S_l and S_l^{\max} are the apparent power and the maximum apparent power of line l .

3.4.3 Constraint on voltage: The node voltage constraint is as follows:

$$U_{i \min} < U_i < U_{i \max} \quad (14)$$

where, U_i is the voltage at node i . $U_{i \max}$ and $U_{i \min}$ are the maximum voltage and minimum voltage, respectively.

3.4.4 Constraints on RE: In the distribution network, nodal voltage can be controlled by PV inverter providing or absorbing reactive power. The RE constraints include reactive capacity and power factor.

$$\begin{cases} P_{DGi,t} = P_{DGi,t}^{MPPT} \\ -\sqrt{S_{DGi}^2 - P_{DGi,t}^2} \leq Q_{DGi,t} \leq \sqrt{S_{DGi}^2 - P_{DGi,t}^2} \\ \cos \phi \leq P_{DGi,t} / S_{DGi} \leq 1 \end{cases} \quad (15)$$

where, $P_{DGi,t}$ and $Q_{DGi,t}$ are the active power and reactive power output of DG i at time t , respectively. $P_{DGi,t}^{MPPT}$ is DG's active power set by maximum power point tracking (MPPT). S_{DGi} is PV inverter capacity at the node i of the network. In the above equations, the reactive capacity of the PV inverter is constrained by both inverter capacity and power factor.

3.4.5 Constraints on ESS: The constraints on ESS are as follows:

(1) State of Charge (SOC)

In the charging/discharging of ESS, the SOC of ESS should not exceed the specified upper and lower limits.

$$E_{SOC, \min} \leq E_{SOC,t} \leq E_{SOC, \max} \quad (16)$$

where, $E_{SOC,t}$ is the SOC of energy storage battery at time t . $E_{SOC, \min}$ and $E_{SOC, \max}$ are the minimum and maximum of SOC, respectively.

(2) Charging/discharging flags

$$\begin{cases} u_{c,t} + u_{d,t} = 1 \\ u_{c,t} \cdot u_{d,t} = 0 \end{cases} \quad (17)$$

where, $u_{c,t}$ and $u_{d,t}$ are the charging and discharging flags at time t , respectively. $u_{c,t} = 1$ when storage charges, while $u_{c,t} = 0$ when ESS does not charge. $u_{d,t} = 1$ when ESS discharges, while $u_{d,t} = 0$ when ESS does not discharge. It should be noted that $u_{c,t}$ and $u_{d,t}$ are modeled as continuous variables in the optimization to simplify the model.

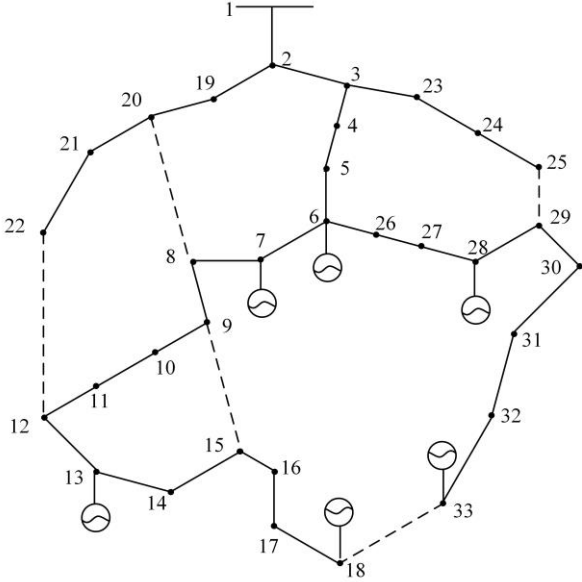


Fig. 3. IEEE 33 node distribution system.

$$\begin{cases} 0 \leq p_{c,t} \leq u_{c,t} p_{c \max} \\ 0 \leq p_{d,t} \leq u_{d,t} p_{d \max} \end{cases} \quad (18)$$

where, $p_{c,t}$ and $p_{d,t}$ are the actual charging and discharging power at time t . $p_{c \max}$ and $p_{d \max}$ are the maximum charging and discharging power.

(3) Recursion of SOC

$$E_{SOC,t+1} = E_{SOC,t} + (u_{c,t} p_{c,t} \eta_c - u_{d,t} \frac{p_{d,t}}{\eta_d}) \Delta t \quad (19)$$

where, η_c is the charging efficiency of ESS and η_d is the discharging efficiency. Δt is the charging/discharging time intervals.

4. Solution methodology

It is important to emphasize that the presented flexibility evaluation model consists of both master problem and subproblem. Moreover, the subproblem includes an upper layer and a lower layer. To solve this problem, the bisection algorithm is adopted to gain maximum feasible deviation, i.e., the boundary point of the feasible region in a particular direction. The master problem searches the critical direction.

4.1. Bisection algorithm for subproblem

The purpose of the subproblem is to identify a maximum feasible deviation, i.e., the boundary point of the feasible region in a particular direction, which is a one-dimensional problem. The bisection algorithm is employed to solve the subproblem. The procedure is as follows:

(1) Initialization.

The expected point of the uncertain region and maximum deviation are denoted as δ_n^0 and δ_u^0 , respectively.

(2) Calculation of Midpoint.

Endpoints at iteration t are represented as δ_n^t and δ_u^t respectively, and the midpoint δ_m^t is obtained by $\delta_m^t = (\delta_n^t + \delta_u^t) / 2$.

(3) Feasibility analysis of midpoint.

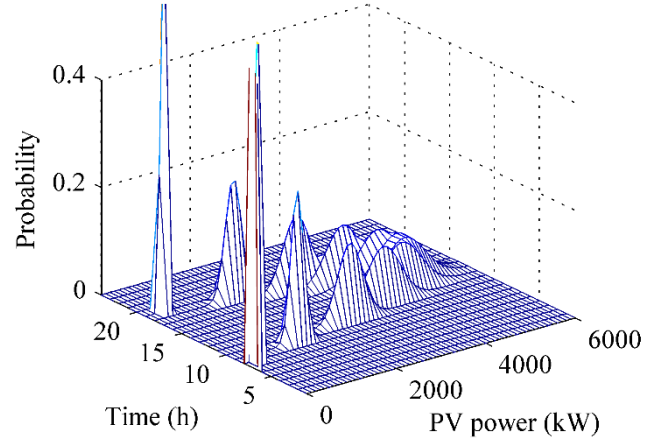


Fig. 4. Sequential probability sequence of the PV.

- ① If δ_m^t is feasible, the boundary point is between δ_m^t and δ_u^t . Thus, $\delta_n^{t+1} = \delta_m^t$ and $\delta_u^{t+1} = \delta_u^t$;
- ② If δ_m^t is infeasible, the boundary point is between δ_n^t and δ_m^t . Thus, $\delta_n^{t+1} = \delta_n^t$ and $\delta_u^{t+1} = \delta_m^t$.
- ④ Repeat (2) and (3) until the algorithm converges, i.e., $|\delta_m^{k+1} - \delta_m^k| \leq \varepsilon$.

The convergence coefficient is defined as ε . The computation accuracy of the bisection algorithm can be enhanced by setting ε to a positive number close to zero.

4.2. Solution process for master problem

The proposed solution process for the master problem comprises the following main steps:

Step 1 Initialization.

- The probability sequences of all uncertain variables are generated.
- The dimension of the sequential direction matrix is set according to the number of time intervals and uncertain variables.

Step 2 Subproblem solution.

The bisection algorithm is utilized to calculate the maximum feasible deviation δ^D in a particular direction D . The procedure of the bisection algorithm is in Section 4.1.

Step 3 Calculation of φ^D .

The probability-weighted maximum feasible deviation φ^D is obtained based on equation (8).

Step 4 Master problem solution.

Repeat Step 2 and Step 3 with different sequential direction matrix, until the optimal solution is obtained.

The master problem is a nonlinear programming (NLP) problem, which is solved by NOMAD solver [31]. NOMAD uses a Mesh Adaptive Direct Search algorithm to solve derivative-free global NLP problems [32]. Because of the convergence coefficient of the bisection algorithm and the computation accuracy of NOMAD, the bias of the bi-level model can be reduced.

5. Case Study

5.1. Introduction of the test system

A modified version of the IEEE 33-node distribution test system [33] is selected for the case study, which is illustrated in Fig. 3. The reference voltage of the case is 12.66kV. The constraint of voltage is set to 0.95p.u. to 1.05p.u., and the branch flow limit of all lines is set to 6.6MVA[34]. PV units

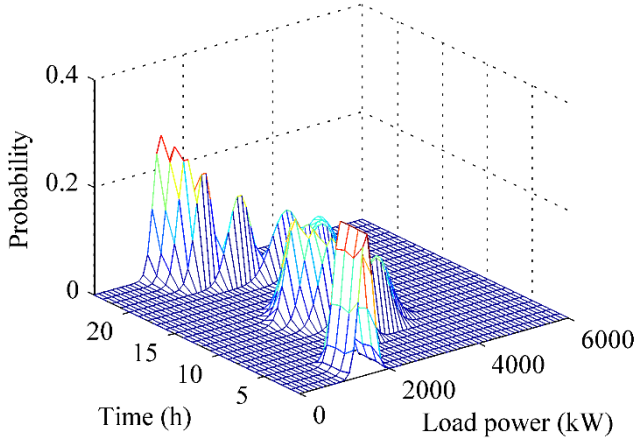


Fig. 5. Sequential probability sequence of the load.

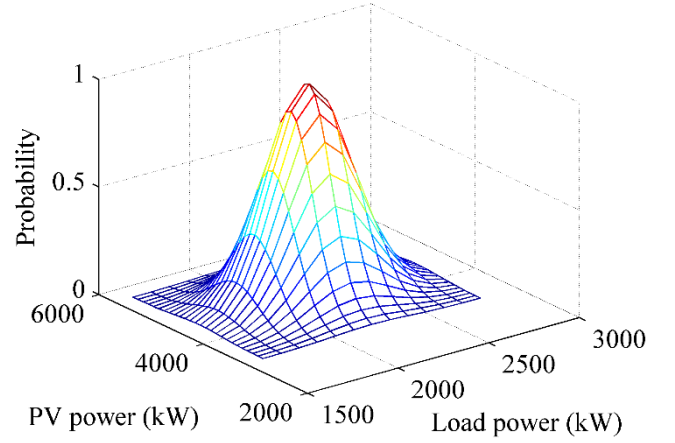


Fig. 7. Probability distribution of uncertain region in weighted flexibility evaluation.

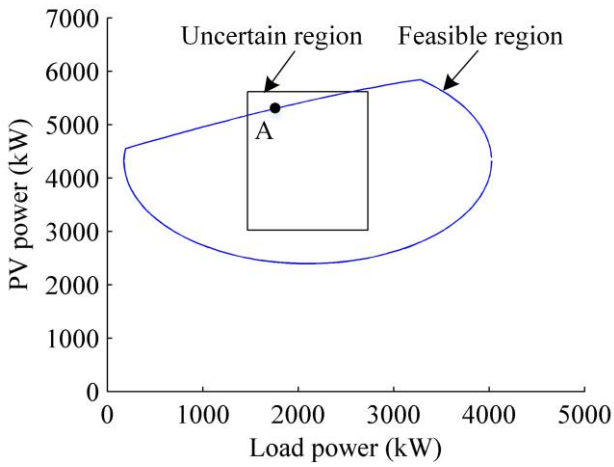


Fig. 6. Feasible region of ordinary flexibility evaluation.

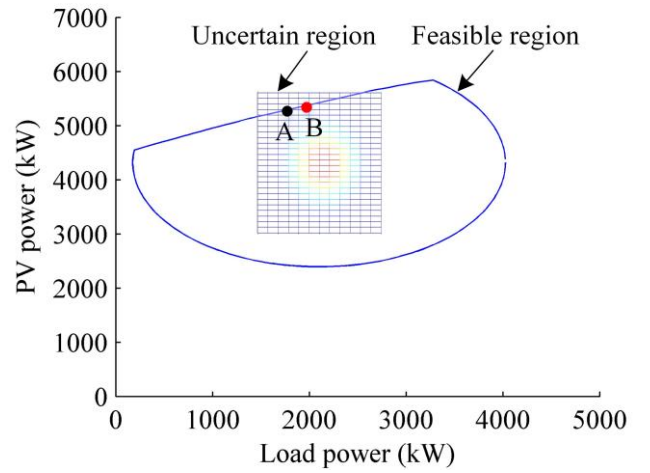


Fig. 8. Feasible region of weighted flexibility evaluation.

are installed at nodes 6, 7, 13, 18, 28, 33, respectively. The installed capacity is 1.2MVA at each node. The minimum power factor of PV inverters is set to be 0.95. ESS is integrated at node 18, with an installed capacity of 0.8MWh. The ESS's maximum charging and discharging power are 240kW and 384kW, respectively [35]. The convergence coefficient ϵ of the bisection algorithm is set to be 10^{-4} .

The standard deviation of PVAP $\delta_{PV}(t)$ is set to be 10% of the predicted value $P_{PV}^N(t)$. Similarly, the standard deviation of load demand is set to be 10% of the predicted value. The sequential probability sequences of PVAP and load demand are given in Fig.4 and Fig.5, respectively. As shown, the PVAP is higher than that of load demand at midday, and this test system is a distribution network with high-penetration RE. The load reactive power changes proportionally to the active power, which is not shown in the figure for simplicity. Based on the uncertain region in one day, the time interval is set to be 1h. For the sake of simplicity, it is assumed that the correlation coefficients between PV output power are 1, and the correlation coefficients between nodal load power are 1 as well. Thus, the uncertain region and feasible region can be presented as a two-dimension figure. All numerical experiment is implemented on MATLAB2016 in a computer with Intel i5-6500 CPU at 3.2GHz, 4GB of RAM.

5.2. Influence of uncertain variables' probability characteristics

In this sub-section, the impact of uncertain variables' probability characteristics on flexibility evaluation is analysed. However, it is complex to analyse in the time scale of one day due to multi-dimension uncertain variables. For simplicity, the flexibility evaluation on one-time point (12:00) is implemented. Weighted flexibility and ordinary flexibility represent the flexibility with and without considering uncertain variables' probability characteristics, respectively. In order to demonstrate the relationship of the uncertain region and the feasible region, the latter is obtained by traversing all the directions at a certain step length (1°) in the two-dimensional uncertain space, because it cannot be directly obtained by solving the proposed model.

5.2.1 Results of flexibility evaluation: Based on the probability sequences of PV and load, the ordinary flexibility and weighted flexibility of the distribution network at 12:00 are evaluated. For a normal distribution with a mean of μ and variance of δ , the probability in the interval $(\mu-3\delta, \mu+3\delta)$ reaches 0.9973. Therefore, $\mu-3\delta$ and $\mu+3\delta$ are selected as the boundary of the uncertain region for both ordinary and weighted flexibility evaluation.

(1) Ordinary flexibility evaluation

The ordinary flexibility of the distribution network at 12:00 is evaluated. The flexibility index is 0.742, and the critical

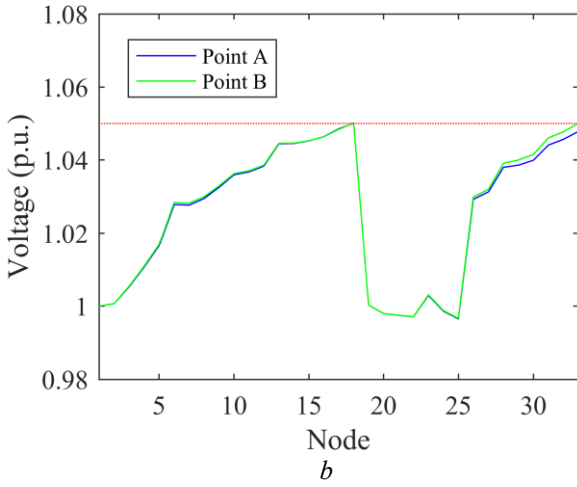
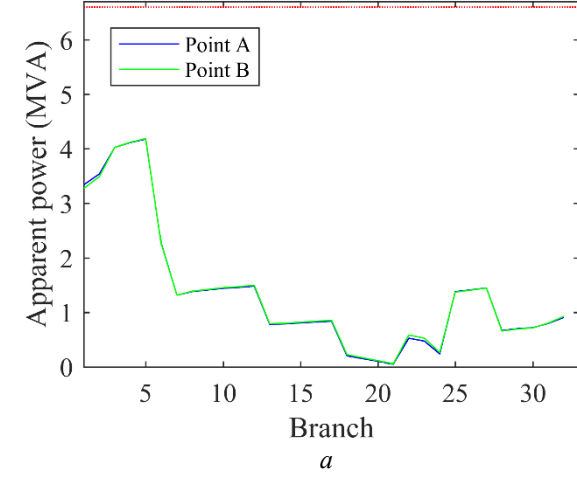


Fig. 9. Branch flow and Node voltage at point A and B (a). Branch flow (b). Node voltage

direction matrix is $(-0.659, 1)$. As shown in Fig.6, the critical point is A, and the feasible region cannot fully cover the uncertain region, indicating that there is a lack of flexibility in the distribution network.

(2) Weighted flexibility evaluation

It is assumed that PV output and load demand are mutually independent of each other. The joint probability distribution of PV output and load demand is shown in Fig.7. Accordingly, the results of weighted flexibility evaluation are depicted in Fig.8.

As seen, there is no difference between the feasible region of weighted flexibility evaluation and the feasible region of ordinary flexibility evaluation. The critical point of weighted flexibility evaluation is point B. However, compared to ordinary flexibility evaluation, the results of weighted flexibility evaluation are different in the following areas:

- The flexibility index is 0.985, larger than that of ordinary flexibility evaluation. The reason is that the area around the expectation point has a higher probability and higher weight, and thus, the weighted flexibility index is larger.
- Critical direction matrix is $(-0.425, 1)$, and the critical point is point B. Specifically, the maximum feasible deviation of point B is 0.756, and the maximum feasible deviation of point A is 0.742. However, the probability of point B is 0.0624, which is higher than the probability of point A,

Table 1 Critical direction matrix of sequential flexibility evaluation

Time	Load	PVAP	Time	Load	PVAP
1	0.0203	0	13	-0.4254	1
2	0.0209	0	14	-0.3482	0.8753
3	0.0218	0	15	-0.2401	0.7012
4	0.0303	0	16	-0.0520	0.1732
5	0.0896	0	17	-0.0529	0.0784
6	0.2117	0	18	0.2741	-0.0929
7	0.2497	0	19	0.6378	-0.2251
8	0.5963	-0.1956	20	0.6702	0
9	0.0181	-0.0151	21	0.0325	0
10	-0.0335	0.1698	22	0.0287	0
11	-0.2335	0.7196	23	0.0266	0
12	-0.3185	0.8217	24	0.0217	0

0.0384. Through equation (8), the probability-weighted maximum feasible deviation of point B is 0.985, and the probability-weighted maximum feasible deviation of point A is 0.990. Therefore, point B is the critical point of the weighted flexibility evaluation.

5.2.2 Active constraints: Based on the PV output and load demand of point A and point B, power flow calculation is performed. Constraints on branch power and nodal voltage are considered as candidates for active constraints.

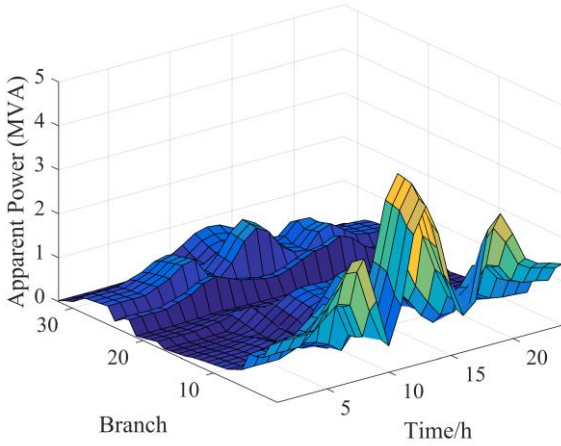
Fig 9(a) represents the apparent power of all branches. As seen, the apparent powers are far from the limit. The maximum apparent power is at Branch 5. This is because there is no PV at node 1~5, and the reverse power will decrease from node 5 to node 1.

The voltages of all nodes are shown in Fig. 9(b). As shown, the voltage of point A is the blue curve and the voltage of point B is the green curve. Considering the probability characteristics of uncertain variables, the active constraints are the voltages of node 18 and node 33. However, the active constraint of ordinary flexibility evaluation is the voltages of node 18. Compared to point A, PV output and load demand of point B are higher, and they share a similar increment. However, PV units are integrated at only 6 nodes. Accordingly, at the nodes with PV units, the increase of PVAP is larger than that of load demand. The voltage of some nodes increases at varying degrees. In ordinary flexibility evaluation, the voltage of node 33 is close to the upper, however, it is an active constraint in the weighted flexibility evaluation. The above results demonstrate the importance of considering PCUV in the flexibility evaluation of distribution networks.

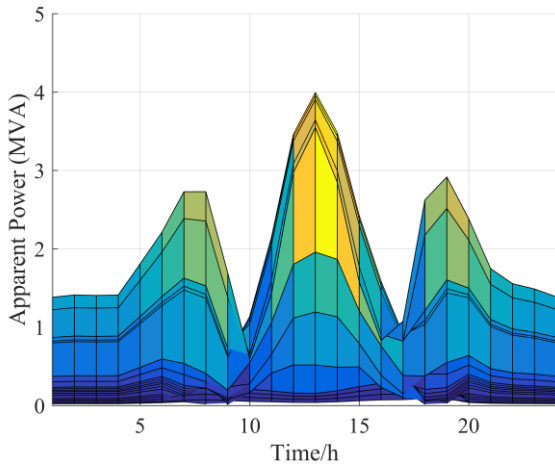
5.3. Sequential weighted flexibility evaluation

In this subsection, the simulation results of sequential weighted flexibility evaluation are presented. The sequential probability sequences of PV output power and load power are depicted in Fig.4 and Fig.5, respectively. The total number of simulation time intervals T is 24h, and the initial SOC of ESS is 0.5.

5.3.1 Results of flexibility evaluation: The result of $F = 0.927$ is obtained, which reveals that the flexible resources cannot satisfy the flexibility requirement in the sequential operation of the distribution network, i.e. there is a lack of



a



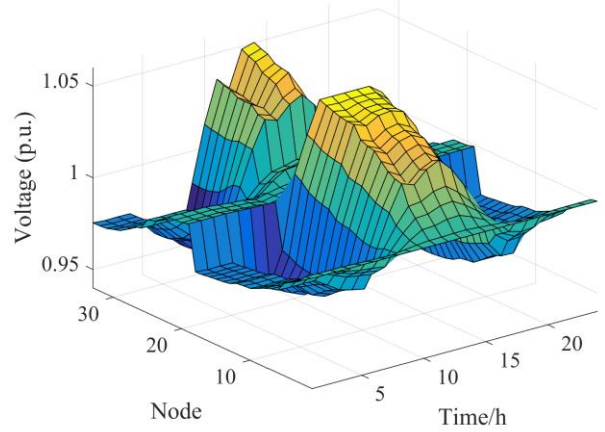
b

Fig. 10. Branch apparent power profiles in 3-D and its projection on the Time- Apparent power plane. (a). Figure in 3-D (b). Projection on the Time- Apparent power plane

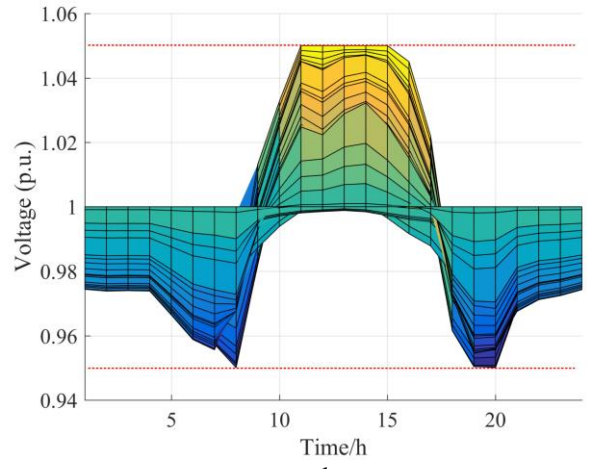
flexibility. The critical direction matrix is represented as follows:

In Table 1, the elements in the critical direction matrix are in bold font. During 1:00~7:00 and 20:00~24:00, the active power output of PV is 0, and consequently, the elements in the corresponding position are 0. However, load is positive. It is because it is more likely to encounter violation against lower bound of voltage and upper bound of branch current due to heavy load.

In sequential weighted flexibility evaluation, larger elements in the critical direction matrix have a greater impact on the flexibility index, which is similar to the critical direction matrix of one-time point. The elements, particularly those of PV at 11:00~15:00, are obviously larger than others. The reason is that the PV output power is significantly higher than load, and the distribution network encounters severe violation against the upper limit of the voltage at this time period. The element “1” appears at 13: 00, which means the problem of voltage violation is more severe than that at 11:00, 12:00, 14:00 and 15: 00. At 7:00 and 19:00. The elements of



a



b

Fig. 11. Voltage profiles in 3-D and its projection on the Time-Voltage plane. (a). Figure in 3-D (b). Projection on the Time-Voltage plane

the load is larger than another time period. This is caused by the violation against lower bound of voltage due to heavy load.

5.3.2 Active constraints: Based on the PV power and load power of the critical point, power flow calculation is performed. Constraints on branch power and node voltage are considered as candidates for active constraints.

The apparent power of all branches is shown in Fig. 10(a). Because it is hard to check whether the branch power is one of the active constraints, the 3-dimensional (3-D) figure is projected to the time-apparent power plane, as shown in Fig. 10(b). As seen, the apparent power of all branches is far from the limit (6.6MVA).

The voltage profiles of all nodes are shown in Fig. 11(a). Fig. 11(b) represents the projection to the time-voltage plane. As seen from Fig. 11(b), the voltages at 8:00, 11:00, 12:00, 13:00, 14:00, 15:00, 19:00, 20:00 are the active constraints that limit the flexibility index. The corresponding elements in the sequential direction matrix are bigger than those in other time. The comparison of Fig. 11 and Table 1 shows that bigger elements of sequential direction matrix indicate the active constraints, i.e., the major cause of flexibility shortage.

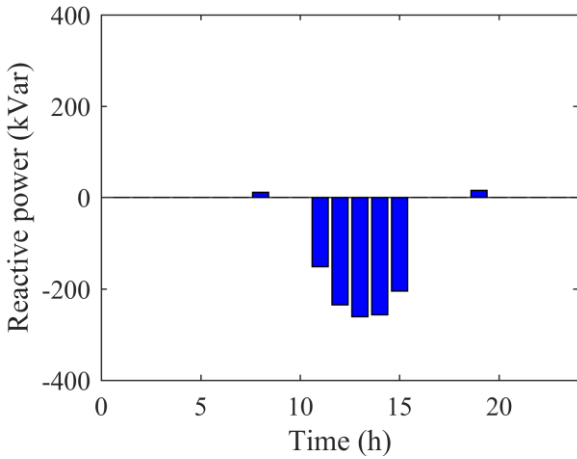


Fig. 12. Reactive output power of the PV inverter at node 18.

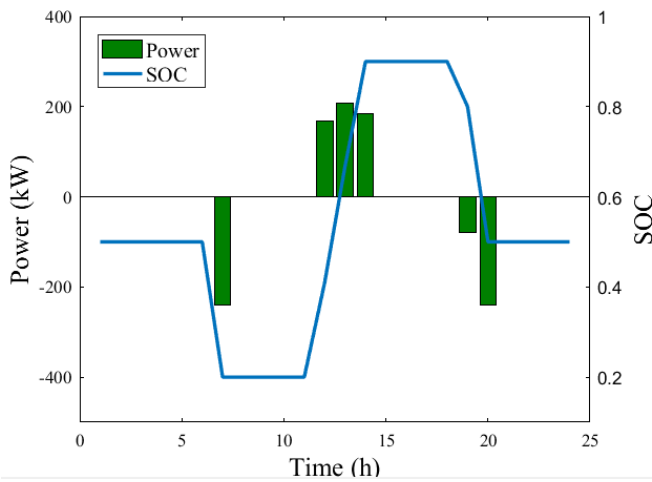


Fig. 13. Charging and discharging power and SOC of ESS.

5.3.3 Decision variables at the critical point: A combination of uncertain variables can be determined according to the critical point. On this basis, the reactive power output of PV inverter at node 18 is shown in Fig.12.

As seen from Fig.12, the main concentration of the output power of PV inverter at node 18 is at 11:00~15:00. The inverter absorbs reactive power to lower the voltage and alleviate the shortage of flexibility.

In Fig.13, there are two vertical axes. The green bars indicate the charging/discharging power of ESS, which are against the left vertical axis. The blue line indicates the SOC of the ESS, which is against the right vertical axis. The ESS discharges at 8:00, 19:00 and 20:00 in order to obtain a higher voltage. However, the ESS charges at 12:00~14:00 to alleviate the voltage violation caused by a high-penetration level of PV units. Constrained by the capacity, the ESS does not charge at 11:00 and 15:00.

The comparison of Fig.11 and Fig.13 provides more insights into the flexibility shortage, which can be used to guide the planning of flexibility resources.

6. Conclusion

In this paper, a novel sequential flexibility evaluation method of active distribution networks is proposed. The

method features a sequential direction matrix and uncertain region with probabilistic characteristics. A bi-level optimization model is formulated based on the feasibility analysis of the uncertain region. According to the simulation results, the weighted flexibility index is larger than the ordinary flexibility index, which reflects the impact of PCUV on flexibility evaluation. In the sequential direction matrix, the corresponding elements of PVAP during midday are obviously larger than other elements, which means the problem of flexibility shortage is mainly caused by PVAP. This research can produce a solid basis for future studies and provide references for the flexibility-oriented scheduling and planning of distribution networks. The future research in flexibility evaluation will consider network flexibility resources such as network reconfiguration and the operation optimization of soft open points.

7. Acknowledgements

This work is supported by the National Key Research and Development Program of China (2016YFB0900400); National Natural Science Foundation of China (NSFC) (51477116).

8. References

- [1] Bahrami, S., Toulabi, M., Ranjbar, S., *et al.*: 'A decentralized energy management framework for energy hubs in dynamic pricing markets', *IEEE Trans. Smart Grid*, 2018, **9**, (6), pp. 6780-6792
- [2] Amini M.H., Nabi B., Haghifam M.R.: 'Load management using multi-agent systems in smart distribution network', Proc. IEEE Power & Energy Society General Meeting, Vancouver, Canada, July, 2013, pp.1-5
- [3] Nunes, J.B., Mahmoudi, N., Saha, T.K., *et al.*: 'Multi-stage co-planning framework for electricity and natural gas under high renewable energy penetration', *IET Gener. Transm. Distrib.*, 2018, **12**, (19), pp. 4284-4291
- [4] Magdy, G., Mohamed, E.A., Shabib, G., *et al.*: 'Microgrid dynamic security considering high penetration of renewable energy', *Protect. Control Mod. Power Syst.*, 2018, **3**, (1), pp. 23-33
- [5] Niu, C., Yang, L., Zhao, J., *et al.*: 'Flexible-regulation resources planning for distribution networks with a high penetration of renewable energy'. *IET Gener. Transm. Distrib.*, 2018, **12**, (18), pp. 4099-4107.
- [6] North American Electric Reliability Corporation, 'Accommodating high levels of variable generation' (North American Electric Reliability Corp, 2009)
- [7] Frew, B.A., Becker, S., Dvorak, M.J., *et al.*: 'Flexibility mechanisms and pathways to a highly renewable US electricity future', *Energy*, 2016, **101**, (8), pp. 65-78
- [8] Eni, R.O., Akinbami, J.F.K.: 'Flexibility evaluation of integrating solar power into the Nigerian electricity grid', *IET Renew. Power Gener.*, 2016, **11**, (2), pp. 239-247
- [9] International Energy Agency, 'Harnessing variable renewables: A guide to the balancing challenge' (Organisation for Economic Co-operation and Development, 2011)
- [10] Nosair, H., Bouffard, F.: 'Flexibility envelopes for power system operational planning', *IEEE Trans. Sustain. Energy*, 2017, **6**, (3), pp. 800-809
- [11] Zhao, J., Zheng, T., Litvinov, E.: 'A Unified Framework for Defining and Measuring Flexibility in Power System', *IEEE Trans. Power Syst.*, 2015, **31**, (1), pp. 339-347
- [12] Muller, F.L., Sundstrom, O., Szabo, J., *et al.*: 'Aggregation of Energetic Flexibility Using Zonotopes', Proc. IEEE Conf. Decision Control, Osaka, Japan, December 2015, pp.1-10
- [13] Muller, F.L., Szabo, J., Sundstrom, O., *et al.*: 'Aggregation and Disaggregation of Energetic Flexibility from Distributed Energy Resources', *IEEE Trans. Smart Grid*, 2019, **10**, (2), pp. 1205-1214
- [14] Olivier, F., Aristidou, P., Ernst, D., *et al.*: 'Active management of low-voltage networks for mitigating overvoltages due to photovoltaic units', *IEEE Trans. Smart Grid*, 2016, **7**, (2), pp. 926-936
- [15] Chen, F., Huang, C., Wang, L., *et al.*: 'Flexibility evaluation of distribution network with high penetration of variable generations'. Proc. IEEE Conf. Energy Internet and Energy System Integration, Beijing, China, November 2017, pp.1-10
- [16] Majzoobi, A., Khodaei, A.: 'Application of Microgrids in Supporting Distribution Grid Flexibility', *IEEE Trans. Power Syst.*, 2017, **32**, (5), pp. 3660-3669
- [17] Ji, H., Wang, C., Li, P., *et al.*: 'Quantified flexibility evaluation of soft open points to improve distributed generator penetration in active distribution

- networks based on difference-of-convex programming', *Appl. Energy*, 2018, **218**, (10), pp. 338-348
- [18] Xiao, J., Wang, Y., Luo, F., *et al.*: 'Flexible distribution network: definition, configuration, operation, and pilot project', *IET Gener. Transm. Distrib.*, 2018, **12**, (20), pp. 4492-4498
- [19] Li, H., Lu, Z., Qiao, Y.: 'Flexibility resource and demand balance mechanism in power system planning considering high penetration of renewable energy', Proc. IEEE Power & Energy Society General Meeting, Chicago, USA, July 2017, pp.1-10
- [20] Lu, Z., Li, H., Qiao, Y.: 'Probabilistic Flexibility Evaluation for Power System Planning Considering its Association with Renewable Power Curtailment', *IEEE Trans. Power Syst.*, 2018, **33**, (3), pp. 3285-3295
- [21] Wan C., Lin J., Guo W., *et al.*: 'Maximum uncertainty boundary of volatile distributed generation in active distribution network', *IEEE Trans. Smart Grid*, 2018, **9**, (4), pp. 2930-2942
- [22] Li, J., Du, J., Zhao, Z., *et al.*: 'An Efficient Method for Flexibility Analysis of Large-scale Nonconvex Heat Exchanger Networks', *Industrial & Engineering Chemistry Research*, 2015, **54**, (43), pp. 10757-10767
- [23] Ulbig, A., Andersson, G.: 'Analyzing operational flexibility of electric power systems', *Int. J. of Electr. Power Energy Syst.*, 2015, **72**, (9), pp. 155-164
- [24] Ulbig, A.: 'Operational flexibility in electric power systems'. PhD thesis, Swiss Federal Institute of Technology Zurich, 2014
- [25] Ji, H., Wang, C., Li, P., *et al.*: 'SOP-based islanding partition method of active distribution networks considering the characteristics of DG, energy storage system and load', *Energy*, 2018, **155**, (14), pp. 312-325
- [26] Chai Y., Guo L., Wang C., *et al.*: 'Network partition and voltage coordination control for distribution networks with high penetration of distributed PV units', *IEEE Trans. Power Syst.*, 2018, **33**, (3), pp. 3396-3407
- [27] Safayet A., Fajri P., Husain I.: 'Reactive power management for overvoltage prevention at high PV penetration in a low-voltage distribution system'. *IEEE Trans. Indus. Appl.*, 2017, **53**, (6), pp. 5786-5794
- [28] Ibrahim, S., Cramer, A., Liu, X., *et al.*: 'PV inverter reactive power control for chance-constrained distribution system performance optimisation'. *IET Gener. Transm. Distrib.*, 2018, **12**, (5), pp. 1089-1098.
- [29] Liu, H., Tang, C., Han, J., *et al.*: 'Probabilistic load flow analysis of active distribution network adopting improved sequence operation methodology', *IET Gener. Transm. Distrib.*, 2017, **11**, (9), pp. 2147-2153
- [30] Kang, C., Yang, G., Xia Q.: 'Development of multidimensional sequence operation theory with applications to risk evaluation in power system generation scheduling' Science in China Series E:Tech Sciences, 2008, **51**, (6), pp. 724-734
- [31] Digabel, S.L.: 'Algorithm 909: NOMAD: Nonlinear Optimization with the MADS Algorithm'. *ACM Trans. Mathematical Software*, 2011, **37**, (4), pp. 1-15
- [32] Qi, J., Huang, W., Sun, K., *et al.*: 'Optimal placement of dynamic var sources by using empirical controllability covariance', *IEEE Trans. Power Syst.*, 2017, **32**, (1), pp. 240-249
- [33] Capitanescu, F., Ochoa, L.F., Margossian, H., *et al.*: 'Assessing the potential of network reconfiguration to improve distributed generation hosting capacity in active distribution systems', *IEEE Trans. Power Systems*, 2015, **30**, (1), pp. 346-356
- [34] Wang S., Chen S., Ge L., *et al.*: 'Distributed generation hosting capacity evaluation for distribution systems considering the robust optimal operation of OLTC and SVC'. *IEEE Trans. Sustain. Energy*, 2016, **7**, (3), pp.1111-1123
- [35] Yoshida, A., Sato, T., Amano, Y., *et al.*: 'Impact of electric battery degradation on cost- and energy-saving characteristics of a residential photovoltaic system', *Energy & Buildings*, 2016, **124**, (15), pp. 265-272